International Geology Review, Vol. 49, 2007, p. 73–89.
Copyright © 2007 by V. H. Winston & Son, Inc. All rights reserved.

Assemblages and Textural Evolution of UHP Eclogites from the Chinese Continental Scientific Drilling Main Hole

LAIXI TONG,[1] BOR-MING JAHN, YOSHIYUKA IIZUKA,
Institute of Earth Sciences, Academia Sinica, Taipei 11529, Taiwan

AND ZHIQIN XU
Institute of Geology, Chinese Academy of Geological Sciences, Beijing 10037, China

Abstract

Coesite-bearing eclogite samples from the Chinese Continental Scientific Drilling main hole (100–2000 m) were examined. Three major evolutionary stages are distinguished from mineral assemblages and textural relations. (1) The pre-peak stage is indicated by inclusion assemblages in rutile eclogite such as amphibole and paragonite, with pre-peak P-T conditions of ~13 kbar and ~910ºC. (2) The peak ultrahigh-pressure (UHP) metamorphic stage is characterized by the mineral assemblage garnet-omphacite-phengite-rutile-apatite-coesite/quartz pseudomorph ± kyanite; P-T conditions reached ~910ºC and ~37 kbar for rutile eclogite, and ~850ºC and ~35 kbar for phengite eclogite. (3) The retrograde stage produced decompression textures via back reactions, such as thin coronas of amphibole or zoisite on garnet, fine-grained amphibole-plagioclase symplectites on omphacite and biotite-plagioclase, or K-feldspar-albite on phengite, ilmenite or titanite on rutile, at P-T conditions of 530–560ºC and 7–9 kbar. The presence of K-feldspar–albite symplectite on phengite and minor interstitial K-feldspar implies that post-peak decompressional partial melting occurred locally during rapid exhumation of the subducted UHP slab.

Two alternative P-T paths may be constructed: (1) the first possesses a different pre-peak stage but similar peak UHP to post-peak decompression cooling for rutile and phengite eclogite; (2) the second shows a consistent evolution from a pre-peak stage via peak UHP stage to a post-peak stage of near-isothermal decompression, followed by near-isobaric cooling for both rutile and phengite eclogite. We prefer the first P-T path, because the inferred paths show a clear increase in pressure and temperature from near-peak to peak UHP stage, and this may be associated with subduction-related tectonism as a result of continental collision between the North China and Yangtze blocks. Rapid subduction and fast retrograde exhumation is likely responsible for preservation of some pre-peak inclusion assemblages and prograde mineral growth zoning.

Introduction

ULTRAHIGH-PRESSURE METAMORPHISM is interpreted to reflect subduction-zone (>27 kbar) conditions under which crustal rocks are transformed at least partially to coesite- and/or diamond-bearing assemblages (Liou et al., 1994; Coleman and Wang, 1995; Liou et al., 1997, 1998, 2004; Ye et al., 2000a). As the recognized largest UHP metamorphic terrane in the world, the Dabie-Sulu metamorphic belt in east-central China formed as a result of continental subduction and collision between the North China and Yangtze blocks (Fig. 1; Liou et al., 1994, 1995; Ernst and Liou, 1995; Hacker et al., 1995; Cong et al., 1996). The Dabie-Sulu UHP terrane includes extensive occurrences of coesite inclusions in garnet, omphacite, and kyanite in eclogite or mafic-ultramafic rock, jadeite in quartzite, dolomite + aragonite in marble (Okay et al., 1989; Wang et al., 1989; Wang and Liou, 1991; Schertl and Okay, 1994; R. Y. Zhang et al., 1995; Liou et al., 1997; Z. Zhang et al., 2000), and coesite inclusions in zircon from orthogneiss (Ye et al., 2000b; Liu et al., 2001). Microdiamond inclusions in garnet in eclogites have also been reported (S. Xu et al., 1992, 2005). Geochronological studies indicate that the UHP metamorphic event occurred during the Triassic (210–230 Ma; e.g., Li et al., 1993; Ames et al., 1996; Chavagnac and Jahn, 1996; Hacker et al., 2000; Jahn et al., 2003a, 2003b; Liu et al., 2004a, 2005). Stable isotope analyses show that some eclogites and associated rocks have

[1]Corresponding author; email: tong@earth.sinica.edu.tw

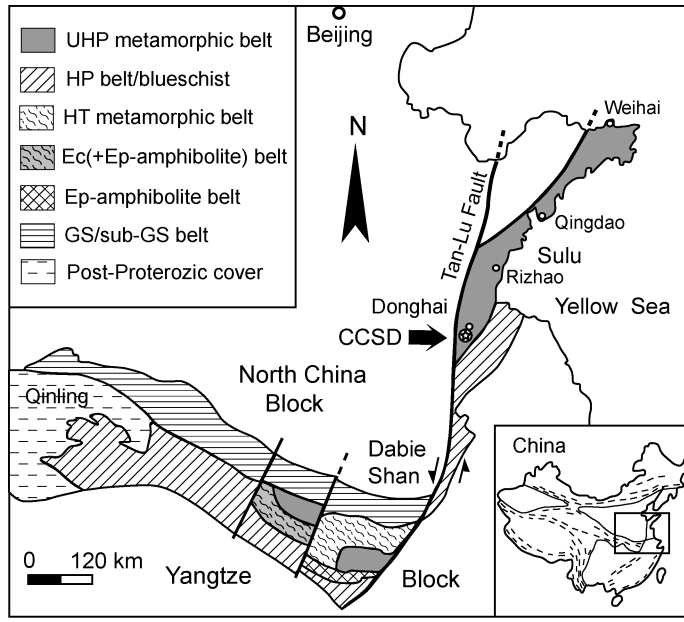


FIG. 1. Regional tectonic units of the Qinling-Dabie-Sulu UHP metamorphic belt in east-central China, showing the location of the main CCSD borehole. Abbreviations: Ec = eclogite; GS = greenschist; HP = high-pressure; UHP = ultra-high-pressure.

unusually low $\delta^{18}O$ values (e.g. –10‰), indicating that their protoliths were altered by meteoric water in a cold climate prior to subduction (Yui et al., 1995; Zheng et al., 1996; Rumble and Yui, 1998).

The record of pre-peak stage for UHP rocks from the Dabie-Sulu terrane has been inferred from prograde growth zoning of garnet and inclusions in peak stage minerals, such as garnet and omphacite (Wang and Liou, 1991; Wang et al., 1992; Enami et al., 1993; Okay, 1993; Cong et al., 1995; R. Y. Zhang et al., 1995; Yang and Jahn, 2000; Z. Zhang et al., 2005). In general, a tight hairpin-style P-T path has been inferred for metamorphic evolution of the UHP rocks (Carswell and Zhang, 2000). However, this type of P-T path may be invalid, and a more open style clockwise P-T path could be more realistic (Carswell and Zhang, 2000). Mineral parageneses and textural relations preserved in UHP eclogites and associated rocks are often used to deduce metamorphic P-T paths, which are critical in the construction of tectonic models. The Chinese Continental Scientific Drilling (CCSD) borehole, located in Donghai of the southern Sulu UHP metamorphic terrane (Fig. 1), provides an excellent chance to study the P-T history of UHP eclogite, with implications for subduction and exhumation processes.

In this work, we examined the mineral assemblages and textural relations of some coesite-bearing rutile and phengite eclogite samples from the CCSD main hole (100–2000 m) in order to understand the P-T evolution of the metamorphic terrane. Preliminary work for the CCSD core samples has been done on general petrography and deformation analysis (Xu et al., 2004; You et al., 2004), geochemistry (Liu et al., 2004b; Z. M. Zhang et al., 2004), and the detailed determination of an inclusion assemblage in zircon (Liu et al., 2002). However, the UHP metamorphic P-T history has not yet been deciphered. Thus, in this study, eclogite samples from the CCSD borehole are selected for further work inasmuch as they preserve parageneses of pre-peak, peak, and retrograde stages and reaction textures, which are particularly appropriate for reconstructing the P-T history.

Geological Setting and CCSD Sample Location

The Sulu UHP metamorphic terrane is the eastern extension of the Qinling-Dabie collision zone, sinistrally displaced to the northeast by the large-scale Tan-Lu fault in eastern China (Fig. 1). The

Sulu belt consists of amphibolite-facies granitic orthogneiss, paragneiss, amphibolite, and marble, in which abundant coesite-bearing eclogite, kyanite quartzite, and UHP garnet peridotite/pyroxenite occur as lenses, layers, or blocks (Hirajima et al., 1990; Yang et al., 1993; R. Y. Zhang et al., 1994, 1995, 2000, 2003; Liou et al., 1995; Cong et al., 1996; Yang and Jahn, 2000). An *in situ* regional UHP metamorphism has been inferred based on the extensive occurrence of coesite inclusions in zircons from country gneiss (Ye et al., 2000b; Liu et al., 2002, 2004a; 2005). U-Pb and Sm-Nd chronology suggests that the UHP metamorphism of the Sulu belt occurred at 220–240 Ma, and the protolith ages of eclogite and country rock are 700–800 Ma (Li et al., 1996; Ames et al., 1996; Hacker et al., 1998; Ayer et al., 2002; Liu et al., 2004a, 2005).

UHP metamorphism of coesite-bearing eclogite in the Sulu UHP terrane has been considered to have occurred at 700–890ºC and 28–40 kbar (R. Y. Zhang et al., 1995; Z. Zhang et al., 2000). However, garnet peridotite and pyroxenite record higher peak P-T conditions of 750–950ºC and 40–65 kbar, as indicated by various P-T calculations and mineral exsolution textures (Yang et al., 1993; Liou et al., 1998; R. Y. Zhang et al., 1994, 2000, 2005; R. Y. Zhang and Liou, 1999; Yang and Jahn, 2000; Ye et al., 2000a). This suggests that UHP metamorphism might have occurred at depths of >180–200 km. Lower pressure inclusion mineral assemblages and prograde garnet growth zonation were preserved in a few eclogites and garnet peridotites, which provide important information of early evolution history (Enami et al., 1993; R. Y. Zhang et al., 1995, 2000; Wallis et al., 1999; Yang and Jahn, 2000). The Sulu eclogites have experienced either granulite- or amphibolite-facies overprinting (Wang et al., 1993; R. Y. Zhang et al., 1995; Cong et al., 1996; Banno et al., 2000; Faure et al., 2001). Thus, different P-T paths are deduced to explain post-peak evolution, with decompression on minor heating (Banno et al., 2000), or minor cooling (Yao et al., 2000; Z. Zhang et al., 2005), or involving an initial stage of isothermal decompression followed by a later stage of near isobaric cooling (Yang, 2004).

A regionally consistent south-dipping mineral stretching lineation is most characteristic in the Sulu terrane. This structural feature is preserved in eclogites and country gneisses; hence it indicates a top-to-the-northwest sense of ductile shear deformation (Faure et al., 2001; Zhao et al., 2003). This is compatible with the southeast-plunging regional mineral elongation lineation in association with a top-to-the-north sense of shear, synkinematic with D2 deformation in the Dabie area (Xue et al., 1996). However, Faure et al. (2001) considered that the top-to-the-northwest ductile deformation was primarily coeval with retrograde amphibolite facies metamorphism, whereas Zhao et al. (2003) suggest that the main ductile shear deformation probably took place under UHP conditions.

A lithological column (0–2000 m) of the main hole of CCSD is shown in Figure 2. The column was divided into four petrotectonic units by Xu et al. (2004): Unit I (0–738 m) is rutile eclogite, with interlayers of ultramafic rock and rare gneiss; Unit II (738–1113 m) is paragneiss, interleaving with some rutile eclogite and minor ultramafic rock; Unit III (1113–1600 m) is granitic orthogneiss, and minor paragneiss; Unit IV (1600–2000 m) is phengite eclogite, with paragneiss and granitic orthogneiss as interlayers.

Petrographic Features

Eighteen eclogite core samples of the present study (Fig. 2) may be divided into rutile and phengite eclogites based on their mineral paragenesis (Xu et al., 2004; You et al., 2004). Representative microphotographs of rutile and phengite eclogites are shown in Figure 3 and Figure 4, including one completely retrograde eclogite in order to demonstrate some aspects of retrograde metamorphism. Mineral abbreviations are after Kretz (1983).

Rutile eclogite

Rutile eclogite mostly occurs in Unit I (0–738 m), in which some traces of early deformation and fabrics were recognized by Xu et al. (2004). N-S–striking, steep east-dipping foliations and horizontal mineral stretching lineations are characteristic. The rutile eclogite is distinguished from phengite eclogite by the presence of abundant rutile (4–5 vol%) as a key component.

Sample B45-a (178 m). This is a weakly retrograded eclogite, and consists mainly of coarse-grained garnet and omphacite, with minor rutile, apatite, quartz, phengite, amphibole, and much less plagioclase, K-feldspar, paragonite, and zoisite. According to the textural equilibrium and the presence of quartz inclusions in garnet with typical radial fractures suggestive of coesite pseudomorphs, the peak UHP assemblage can be inferred as garnet-omphacite-rutile-apatite-phengite-coesite. The pre-

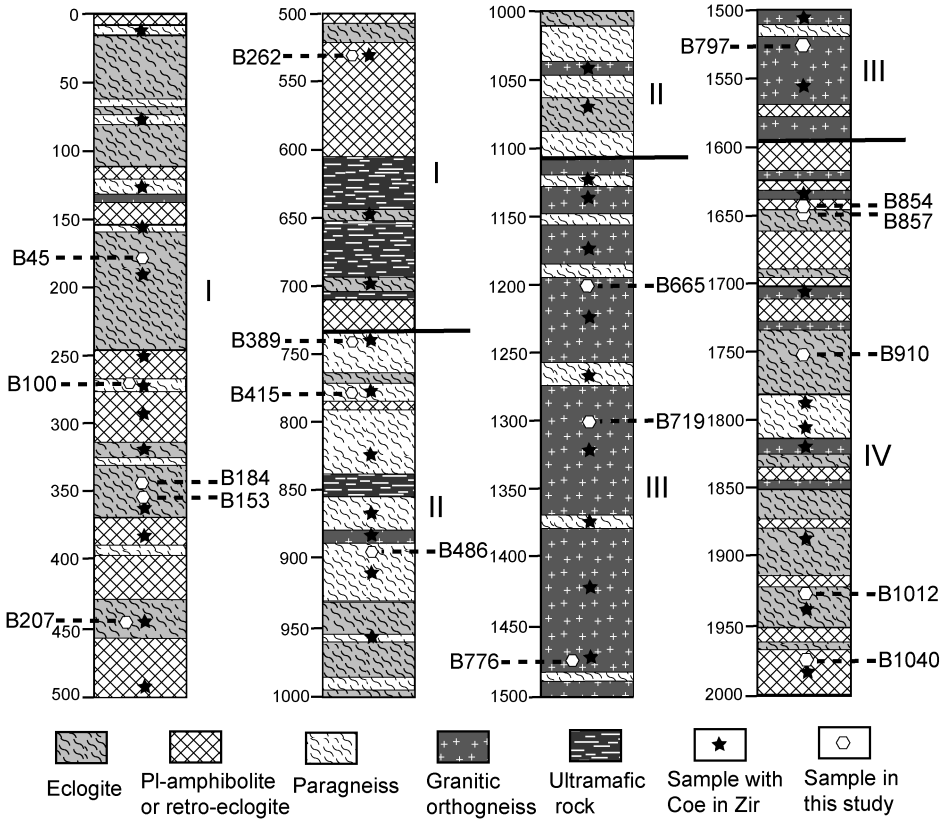


FIG. 2. Lithological column (0–2000 m) of the main CCSD borehole in Donghai, eastern China, showing core sample locations in this study and those with zircons containing coesite inclusions (after Liu et al., 2004b; Xu et al., 2004).

peak prograde assemblage is inferred from inclusions preserved in peak coarse-grained garnet and clinopyroxene grains. For instance, small euhedral amphibole grains occur as inclusions in garnet (Fig. 3A), whereas an amphibole inclusion together with a garnet occurs in a coarse-grained clinopyroxene with extensive fractures (Fig. 3B). This texture suggests prograde dehydration reaction as follows:

$$\text{Amp} \rightarrow \text{Grt} + \text{H}_2\text{O}. \quad (1)$$

Apatite, rutile, and phengite inclusions are also present in coarse-grained garnet (Figs. 3C and 3D). Given the observed consistent fabrics in garnet grains in association with D2 deformation, the fabric is thus inferred as S2 (Fig. 3C). In addition, a fine-grained paragonite flake occurs as an inclusion in a coarse clinopyroxene grain, and implies another possible prograde dehydration reaction as follows:

$$\text{Pg} \rightarrow \text{Jd (in Cpx)} + \text{H}_2\text{O}. \quad (2)$$

Thus, pre-peak prograde assemblage may be inferred as amphibole and paragonite.

The post-peak assemblage is defined by the interstitial K-feldspar–quartz assemblage (Fig. 3E) and corona or symplectite assemblages after peak mineral grains. For example, amphibole-plagioclase symplectite replaced clinopyroxene and amphibole surrounded garnet (Fig. 3F), suggesting a retrograde back reaction (Ernst and Liou, 2000) as follows:

$$\text{Grt} + \text{Cpx} + \text{H}_2\text{O} \rightarrow \text{Amp} + \text{Pl}. \quad (3)$$

Zoisite coronas on garnet grains and biotite-plagioclase symplectite on phengite flakes are also present. They suggest the following post-peak back reactions, respectively:

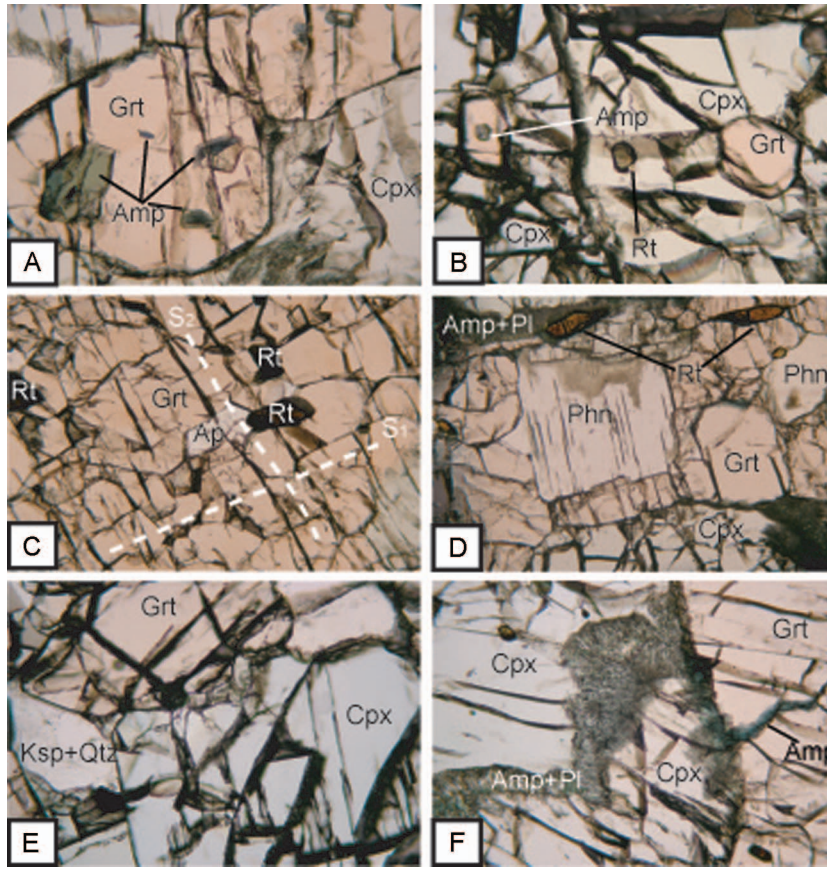


FIG. 3. Microphotographs for sample B45-a (rutile eclogite), showing mineral assemblages and textural relations. A. Euhedral amphibole inclusions in a garnet grain. B. Rutile and garnet inclusions in a clinopyroxene grain, and small amphibole in a garnet, which, in turn, occurs as an inclusion in clinopyroxene. C. Coarse-grained garnet grain with inclusions of apatite and rutile. D. Phengite inclusion in garnet grain, fine-grained amphibole-plagioclase symplectite on clinopyroxene, and thin ilmenite rim on rutile grain. E. Interstitial K-feldspar-quartz assemblage between garnet and clinopyroxene grains. F. Fine-grained amphibole-plagioclase symplectite on clinopyroxene and amphibole rim along fractures in garnet. All the field of view (width) is 1.2 mm except that Figure 3C is 1.8 mm and Figure 3E is 2.2 mm.

$$\text{Grt} + \text{H}_2\text{O} \rightarrow \text{Zo}; \quad (4)$$

$$\text{Phn} \rightarrow \text{Bt} + \text{Pl}. \quad (5)$$

In addition, rutile is typically rimmed by ilmenite, and apatite develops fine pyrite exsolution rods/needles in preferred orientation. These textures may reflect rapid retrograde decompression.

Sample B262-d (533 m). The sample is a weakly to strongly retrograded eclogite, composed mainly of garnet and clinopyroxene, with minor rutile, phengite, pyrite, and apatite. Assemblages and textures are similar to those of sample B45-a. This sample is characterized by a preferred alignment of peak assemblages, whereas the clinopyroxene grains show strong elongation and ductile deformation. In the weakly retrograde zone, garnet grains contain pseudomorphs after coesite with radial fractures (Fig. 4A), or very fine grained coesite, rutile, and clinopyroxene inclusions (Fig. 4B). The coesite pseudomorphs suggest the coesite-quartz transformation reaction during initial post-peak decompression:

$$\text{Coe} \rightarrow \text{Qtz}. \quad (6)$$

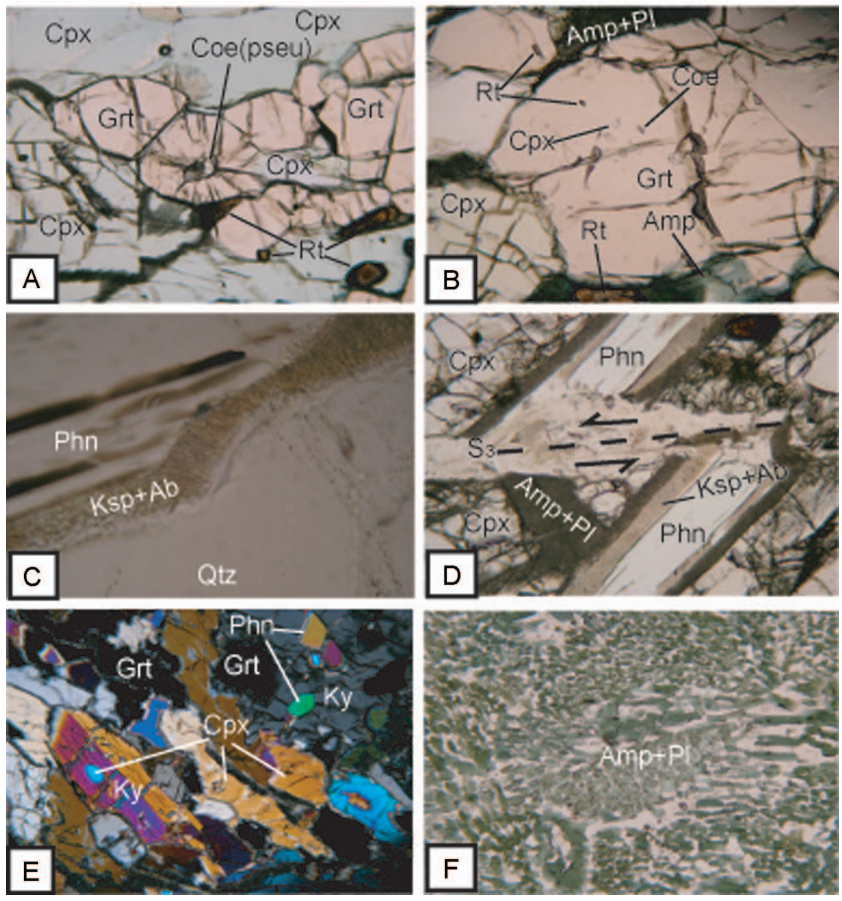


FIG. 4. Microphotographs for rutile eclogite sample B262-d; phengite eclogite samples B1012-e, B854-a, and B857-a; and strongly retrograded eclogite sample B389-d. A. Sample B262-d, coesite pseudomorph in garnet grain with radial fractures. B. Sample B262-d, fine-grained coesite, rutile, and clinopyroxene inclusions in garnet grain. C. Sample B854-a, fine-grained K-feldspar-albite symplectite on phengite grain. D. Sample B857-a, sinistral micro-scale fault displacement, with amphibole-plagioclase symplectite on clinopyroxene grain, and K-feldspar-albite symplectite on phengite grain. E. Sample B1012-e, phengite and clinopyroxene inclusions in kyanite grain. F. Sample B389-d, complete retrograde eclogite with a dominant assemblage of amphibole and sodic plagioclase. The field view (width) in Figures 4A and 4E is 2.4 mm, and that in Figures 4B and 4D is 1.8 mm, whereas the field of view in Figs. 4C and 4F is 0.4 mm and 1.8 mm, respectively.

Similar to sample B45-a, retrograde symplectite assemblages of biotite-plagioclase on phengite flakes, amphibole-plagioclase on clinopyroxene grains, and thin coronas of amphibole on garnet grains and ilmenite on rutile grains are also present. However, in the strongly retrograded zone, clinopyroxene grains have been replaced by a fine-grained secondary clinopyroxene-plagioclase assemblage, with only preservation of the pseudomorphed texture of clinopyroxene grains. This texture may have formed through a post-peak decompression metamorphic reaction as follows:

$$\text{Cpx1} \rightarrow \text{Cpx2} + \text{Pl}. \qquad (7)$$

A similar texture has been described by Yang (2004) from the southern Sulu region, which was interpreted to have been formed via metasomatism as a result of fluid activity along grain boundaries.

Phengite eclogite

Phengite eclogite is the principal rock type of Unit IV (1600–2000 m). The presence of abundant phengite and minor fine-grained rutile is characteristic. Some parallel-aligned phengite flakes are inferred to represent an early foliation by You et al. (2004), whereas strongly elongated garnet and omphacite grains lying in the foliation plane suggest that peak UHP metamorphism was synchronous with compression structures. Due to abundant phengite, the protolith of the phengite eclogite is inferred to be crust-derived (e.g., You et al., 2004).

Sample B854-a (1645 m). This is a weakly retrograde eclogite, composed of garnet, omphacite, and phengite, with minor rutile, apatite, quartz, K-feldspar, and trace amphibole and albite. The peak assemblage is Grt + Omp + Phn + Rt + Ap. The coarse-grained garnet and omphacite are elongated and show ductile deformation, whereas phengite flakes display kinks, and show undulose extinction, probably resulting from ductile deformation. Occasionally, in low strain bands, some coarse phengite flakes show optical zoning with the development of a fine-grained symplectite assemblage of K–feldspar-albite (Fig. 4C). This texture could have formed as a result of post-peak decompressional partial melting (Harley and Carswell, 1995; Ye et al., 2001), through a reaction of:

$$\text{Phn} + \text{Qtz} \rightarrow \text{Ksp} + \text{Ab} + \text{H}_2\text{O}. \qquad (8)$$

Garnet is rimmed by amphibole, and omphacite is replaced by fine-grained symplectite of Amp+Pl at the grain margin, suggesting that the rock also underwent retrograde metamorphism described by reaction (3). In addition, fine-grained rutile shows thin ilmenite coronas in the rim, and ilmenite exsolution in rutile.

Sample B857-a (1649 m). This sample has an assemblage and textural feature similar to sample B854-1. However, a sinistrally sheared brittle fracture zone is developed across the entire fabric of sample B857-a (Fig. 4D). Because the major fabric preserved in coarse clinopyroxene grains might have formed as a result of D2 deformation, the shear band infilled by calcite-dominated retrograde minerals indicates a late retrograde fabric consistent with an S3 foliation.

Sample B1012-e (1929 m). The sample is a weakly retrograde kyanite-bearing phengite eclogite. The peak assemblage is inferred as garnet-omphacite-phengite-kyanite-apatite from equilibrated textural relationships. Rutile normally occurs as very fine grained inclusions in garnet grains. Garnet, omphacite, and phengite show ductile deformation. Some coarse-grained kyanite grains exhibit simple twinning, and contain omphacite or phengite inclusions (Fig. 4E). The texture suggests a possible prograde reaction as follows:

$$\text{Cpx1} + \text{Phn} \rightarrow \text{Grt} + \text{Ky} + \text{Cpx2} + \text{H}_2\text{O}. \qquad (9)$$

Similarly, the development of a thin amphibole corona on garnet, fine-grained symplectite of amphibole-plagioclase on omphacite, and K-feldspar-albite on phengite may be the result of retrograde reactions.

Completely retrograded eclogite

Eclogititic minerals in extensively retrograded eclogite have been completely replaced by amphibolite-facies mineral assemblages. The rock looks like a gneiss without any relics of UHP minerals.

Sample B389-d (741 m). This sample occurs as a thin layer within the paragneiss at the top of Unit II of the CCSD lithological column (Fig. 2). It is mainly composed of amphibole and plagioclase, with minor epidote, biotite, quartz, titanite, and accessary zircon. The contour shape of Amp + Pl intergrowths indicates that it is a pseudomorph after omphacite or garnet (Fig. 4F). Coesite inclusions in zircon suggest that this rock experienced UHP metamorphism (Liu et al., 2003). Completely retrograded eclogites with similar assemblages and textural features from the Dabie UHP terrane have also been reported by R. Y. Zhang et al. (2003), and the transformation from quartz eclogite to gneiss was attributed to fluid infiltration and metasomatism along grain boundaries and fractures during the retrograde stage.

Mineral Chemistry

Mineral composition analyses were undertaken on a JEOL JXA-8900R electron microprobe at the Institute of Earth Sciences, Academia Sinica. Working conditions were 10-nA electron beam current, and an accelerating voltage of 15 kV. The results of typical mineral compositions for the CCSD core samples B45-a and B854-a are listed in Table 1.

Garnet

An increase of the X_{Mg} (= $Mg/Mg + Fe^{2+}$) value in a garnet grain from core to rim is usually considered as growth zonation resulting from prograde metamorphism. For both rutile and phengite eclogites

TABLE 1. Microprobe Analyses of the Main Minerals in Rutile Eclogite (Sample B45-a) and Phengite Eclogite (Sample B854-a) from the CCSD Borehole in Donghai[1]

	B45-a													B854-a							
	Grt(i)	Cpx(c)	Amp(i)	Pg(i)	Grt(c)	Grt(r)	Cpx(c)	Cpx(r)	Amp(s)	Pl(s)	Ksp(i)	Phn1	Phn2	Grt	Cpx	Grt(c)	Grt(r)	Cpx(c)	Cpx(r)	Phn1	Phn2
SiO_2	39.30	56.93	37.33	45.89	38.68	39.29	56.48	56.64	48.86	65.29	64.61	50.40	53.34	40.41	57.16	39.41	39.43	56.97	57.02	51.98	53.71
TiO_2	0.00	0.01	0.09	0.20	0.02	0.00	0.06	0.03	0.14	0.03	0.05	0.41	0.44	0.08	0.09	0.10	0.01	0.00	0.09	0.45	0.39
Al_2O_3	21.71	10.84	19.30	38.02	20.86	21.91	10.74	11.09	8.54	21.56	17.48	23.92	22.05	20.88	11.69	22.42	22.13	11.83	12.27	25.01	22.88
Cr_2O_3	0.03	0.01	0.01	0.00	0.01	0.03	0.00	0.04	0.03	0.04	0.00	0.10	0.00	0.00	0.04	0.05	0.02	0.04	0.03	0.04	0.00
Fe_2O_3	0.00	0.00	0.89	0.00	1.35	0.00	0.00	0.00	0.00	0.51	0.06	0.00	0.00	0.32	0.00	0.00	1.22	0.00	0.00	0.00	0.00
FeO	23.31	5.85	18.30	0.83	22.20	23.17	5.70	5.66	10.75	0.00	0.00	2.43	2.26	20.84	3.56	22.04	19.52	3.56	3.37	1.68	1.37
MnO	0.57	0.00	0.31	0.00	0.54	0.48	0.03	0.00	0.08	0.00	0.00	0.00	0.05	0.37	0.06	0.69	0.46	0.08	0.00	0.00	0.00
MgO	3.63	5.96	5.24	0.14	3.50	4.04	6.22	5.80	9.12	0.05	0.00	3.06	3.54	7.88	8.21	6.44	8.13	7.94	7.95	4.29	4.86
CaO	11.62	12.57	11.26	0.40	13.19	11.42	12.35	12.26	17.47	2.82	0.00	0.00	0.00	10.06	12.18	9.42	9.90	12.58	12.54	0.00	0.03
Na_2O	0.03	6.95	3.24	7.10	0.07	0.05	7.33	7.15	2.81	9.47	0.00	0.25	0.13	0.04	6.15	0.00	0.00	6.06	5.79	0.31	0.17
K_2O	0.02	0.00	0.18	0.34	0.02	0.01	0.00	0.00	0.04	0.06	16.77	10.70	11.00	0.02	0.05	0.00	0.00	0.05	0.00	10.77	10.56
Totals	100.22	99.25	96.15	92.92	100.43	100.40	98.92	98.68	96.84	99.83	99.11	91.28	92.82	100.90	99.19	100.58	100.83	99.11	99.07	94.54	93.98
O	12	6	23	11	12	12	6	6	23	8	8	11	11	12	6	12	12	6	6	11	11
Si	3.044	2.043	5.776	3.009	3.009	3.033	2.036	2.042	7.200	2.875	3.021	3.520	3.651	3.059	2.024	3.005	2.978	2.021	2.017	3.489	3.607
Ti	0.000	0.002	0.010	0.010	0.001	0.000	0.002	0.001	0.015	0.001	0.002	0.022	0.023	0.005	0.002	0.006	0.001	0.000	0.002	0.023	0.020
Al	1.983	0.459	3.521	2.939	1.913	1.994	0.456	0.471	1.483	1.119	0.964	1.969	1.779	1.863	0.488	2.015	1.971	0.495	0.512	1.979	1.811
Cr	0.002	0.002	0.001	0.000	0.001	0.002	0.000	0.001	0.003	0.001	0.000	0.006	0.000	0.000	0.001	0.003	0.001	0.001	0.001	0.002	0.000
Fe^{3+}	0.000	0.000	0.104	0.000	0.079	0.000	0.000	0.000	0.000	0.017	0.002	0.000	0.000	0.018	0.000	0.000	0.070	0.000	0.000	0.000	0.000
Fe^{2+}	1.510	0.176	2.368	0.046	1.444	1.496	0.172	0.171	1.328	0.000	0.000	0.142	0.129	1.319	0.105	1.405	1.233	0.106	0.100	0.094	0.077
Mn	0.037	0.000	0.041	0.000	0.036	0.031	0.001	0.000	0.010	0.000	0.000	0.000	0.003	0.024	0.002	0.045	0.029	0.002	0.000	0.000	0.000
Mg	0.419	0.319	1.208	0.014	0.406	0.465	0.334	0.312	2.002	0.003	0.000	0.318	0.361	0.889	0.433	0.732	0.915	0.420	0.419	0.429	0.486
Ca	0.965	0.483	1.867	0.028	1.099	0.945	0.477	0.474	2.599	0.133	0.000	0.000	0.000	0.816	0.462	0.770	0.802	0.478	0.475	0.000	0.002
Na	0.005	0.484	0.972	0.903	0.011	0.007	0.513	0.500	0.802	0.809	0.012	0.034	0.017	0.006	0.422	0.000	0.000	0.417	0.398	0.040	0.022
K	0.002	0.000	0.036	0.028	0.002	0.001	0.000	0.000	0.008	0.003	1.001	0.954	0.962	0.002	0.002	0.000	0.000	0.002	0.000	0.923	0.906
Sum	7.967	3.967	15.904	6.977	8.000	7.974	3.991	3.971	15.447	4.961	5.001	6.965	6.926	8.000	3.942	7.981	8.000	3.941	3.923	6.980	6.931
X_{Mg}	0.217	0.644	0.338		0.219	0.237	0.660	0.646	0.601			0.691	0.737	0.403	0.805	0.343	0.426	0.798	0.807	0.820	0.863
X_{Ca}	0.329				0.368	0.322								0.268		0.261	0.269				
Jd		47.5					46.1	48.4							55.2			55.3	58.6		
X_{Al}		0.230					0.228	0.236							0.244			0.248	0.256		

[1]Abbreviations: Grt(i) = garnet inclusion in clinopyroxene; Cpx(c) = clinopyroxene core; Amp(i) = amphibole inclusion in garnet; Pg(i) = paragonite inclusion in garnet; Grt(c) = garnet core; Grt(r) = garnet rim; Cpx(r) = clinopyroxene rim; Amp(s) and Pl(s) = amphibole and plagioclase in symplectite, respectively, on clinopyroxene; Ksp(i) = interstitial K-feldspar; Phn1 = phengite core; Phn2 = phengite rim.

from the CCSD borehole, garnet grains exhibit an increase of X_{Mg} from the core to rim. The X_{Mg} value of rutile eclogite sample B45-a increases from 0.219 in the core to 0.237 in the rim, whereas the X_{Ca} value (= Ca/Mg + Fe^{2+}+Ca+Mn) decreases from 0.368 in the core to 0.322 in the rim (Table 1). The garnet inclusion in coarse-grained clinopyroxene for sample B45-a has an X_{Mg} of 0.217, similar to that of garnet core, but an X_{Ca} of 0.329 between the core and rim. Likewise, for phengite eclogite sample B854-a, X_{Mg} increases from 0.343 in the core to 0.426 in the rim, whereas X_{Ca} increases slightly from 0.261 in the core to 0.269 in the rim. For sample B854-a, the garnet core contains a higher TiO_2 (0.10 wt%) than the garnet rim (0.01 wt%; Table 1).

In addition, supersilicic garnet is often called majoritic garnet and interpreted as formed under UHP conditions (e.g., R. Y. Zhang and Liou, 1999). Majoritic garnet has been used to infer UHP conditions during continental deep subduction (Ye et al., 2000a; R. Y. Zhang et al., 2005).. R. Y. Zhang et al. (2005) reported supersilicic garnet of very high Si content (up to 3.058 per formula unit) in eclogite from the Yangkou ultramafic complex, and interpreted the presence of a majorite component. In this study, a garnet inclusion in coarse clinopyroxene in sample B45-a has a high Si content of 3.044 p.f.u., whereas a small garnet grain in sample B854-a shows an even higher Si content of 3.059 p.f.u. (Table 1). They are similar to the supersilicic garnet reported by R. Y. Zhang et al. (2005). This confirms that peak metamorphism in the southern Sulu region reached UHP conditions.

Clinopyroxene

Clinopyroxene is omphacitic, and the jadeite component was calculated on the basis of Jd = Al^{VI}/(Na+Ca) (Liou et al., 1997). The jadeite component generally increases from core to rim. For sample B45-a, it increases from 46.1 in the core to 48.4 in the rim (Table 1). Accordingly, its X_{Al} (=Al/2 per 6 oxygen) value increases from 0.228 in the core to 0.236 in the rim, whereas X_{Mg} decreases from 0.660 in the core to 0.646 in the rim. For sample B854-a, the jadeite component increases from 55.3 in the core to 58.6 in the rim. The X_{Al} value increases from 0.248 in the core to 0.256 in the rim, whereas the X_{Mg} value shows a slight increase from 0.798 in the core to 0.807 in the rim.

Phengite

The Si content in eclogitic phengite is an indicator of metamorphic pressure. In the southern Sulu UHP terrane, high-Si phengite has been suggested to have formed at peak UHP stage (e.g. Z. Zhang et al., 2005). A small amount of coarse-grained phengite flakes are also recognized in rutile eclogite. For sample B45-a, phengite has a high Si value of 3.52 p.f.u. (O = 11) in the core, and 3.65 p.f.u. in the rim (Table 1). Peak phengite flakes are more abundant in the phengite eclogite. For sample B854-a, the Si value in phengite indicates a similar variation with an increase from the core (3.49 p.f.u.) to the rim (3.61 p.f.u.).

Amphibole

Amphibole occurs as pre-peak stage inclusions in coarse-grained garnet or as a retrograde symplectitic phase after omphacite. For sample B45-a, according to the nomenclature of amphiboles of Leake et al. (1997), amphibole inclusions in garnet are ferro-edenite and ferro-pargasite. They have a lower SiO_2 content (37.33 wt%) and a higher Al_2O_3 content (19.30 wt%) than symplectitic magnesiohornblende (48.86 wt% and 8.54 wt%). Accordingly, the amphibole inclusion in garnet has a much lower X_{Mg} value of 0.338 than that (0.601) of symplectitic hornblende. A small euhedral amphibole inclusion in garnet is similar in composition to the mantle-derived amphibole reported by R. Y. Zhang et al. (2005).

Other minerals

Paragonite (Pg) occurs as a fine-grained flake inclusion in a coarse clinopyroxene grain in sample B45-a, with a Na_2O content of 7.10 wt%. Plagoclase occurs mainly as retrograde phase in symplectite assemblages, and contains a considerable amount of CaO (Ca/Ca+Na = 0.14) in sample B45-a. K-feldspar occurs as interstitial phase between garnet and clinopyroxene in sample B45-a, and is nearly pure K-feldspar.

P-T Estimates and Possible P-T Paths

The inferred texturally equilibrated mineral assemblages constrain the metamorphic P-T conditions for pre-peak prograde stage, peak UHP stage, and retrograde stage. Possible P-T paths of rutile and phengite eclogites are derived from the P-T estimates of different metamorphic stages listed in Table 2.

TABLE 2. P-T Estimates for Pre-Peak, Peak, and Post-Peak Assemblages for Rutile Eclogite (Sample B45-a) and Phengite Eclogite (Sample B854-a) for the CCSD Borehole in Donghai[1]

Sample B45 (pre-peak)

P (kbar)		
JR	HZ	H
11.4	13.8	15.1

T (°C)	
GP	(1132)
Pe	910

Sample B45-a (near-peak)

	P (kbar)		
T (°C)	700	750	800
MS	29.3	29.7	30.2

Sample B45-a (peak)

	P (kbar)		
T (°C)	700	750	800
MS	35.0	35.8	36.3

Sample B45-a (near-peak)

	T (°C)		
P (kbar)	25.0	30.0	35.0
P	855	869	882
K	851	866	882
PN	816	844	871

Sample B45-a (peak)

	T (°C)		
P (kbar)	30.0	35.0	40.0
P	897	911	925
K	898	914	930
PN	888	915	943

Sample B45-a (post-peak)

	T (°C)		
P (kbar)	7.0	8.0	9.0
BH	560	547	534

Sample B854-a (near-peak)

	P (kbar)		
T (°C)	700	750	800
MS	27.8	28.3	28.7

Sample B854-a (peak)

	P (kbar)		
T (°C)	700	750	800
MS	33.3	33.8	34.2

Sample B854-a (near-peak)

	T (°C)		
P (kbar)	25.0	30.0	35.0
P	752	765	779
K	739	754	769
PN	700	727	755

Sample B854-a (peak)

	T (°C)		
P (kbar)	30.0	35.0	40.0
P	862	877	891
K	861	877	893
PN	752	780	807

[1]Abbreviations: H = Hollister et al., 1987; HZ = Hammarstrom and Zen, 1986; JR = Johnson and Rutherford, 1989; GP = Graham and Powell, 1984; Pe = Perchuk et al., 1985; MS = Massonne and Schreyer, 1989; P = Powell, 1985; K = Krogh, 1988; PN = Pattison and Newton, 1989; BH = Blundy and Holland, 1990.

Pre-peak prograde stage (I)

Inclusion assemblages and mineral compositions allow determination of P-T conditions for the pre-peak metamorphic stage. For the rutile eclogite sample B45-a, fine-grained euhedral amphibole inclusions in garnet produced an average pressure of ~13 kbar via the Al-in amphibole barometers (Hammarstrom and Zen, 1986; Hollister et al., 1987; Johnson and Rutherford, 1989). The corresponding temperature of ~910ºC was obtained from the amphibole composition and composition of the garnet core in contact with amphibole via the Grt-Amp thermometer of Perchuck et al. (1985). This temperature is considered more reasonable than an anormously high T estimate (1132 ºC) produced using the Grt-Amp thermometer of Graham and Powell (1984) (Table 2). The temperature estimate of ~910 ºC is consistent with the hypothesis that the amphibole inclusion in garnet was mantle-derived, and may be stable up to ~900 ºC at upper mantle conditions (Ernst, 1999).

Peak UHP stage (II)

P-T conditions for the peak UHP metamorphic stage are calculated from the core and rim compositions of minerals of prograde growth zonation, in which reference pressures are produced using the phengite Si barometer of Massone and Schreyer (1989). For rutile eclogite sample B45-a, a near-peak reference pressure is estimated at ~30 kbar from a low-Si phengite core composition, whereas a peak reference pressure of ~37 kbar is yielded from a high-Si phengite rim composition (Table 2). The garnet core and clinopyroxene core compositions produced a near-peak temperature of ~860ºC at ~30 kbar, and a Grt (rim)-Cpx (rim) pair yielded a consistent peak temperature estimate of ~910ºC at ~35 kbar from the Grt-Cpx thermometers of Powell (1985), Krogh (1988), and Pattison and Newton (1989).

For phengite eclogite sample B854-a, a near-peak reference pressure is estimated as ~28 kbar from a low-Si phengite core composition, whereas a peak reference pressure of ~35 kbar is yielded from a high-Si phengite rim composition (Table 2). A near-peak temperature of ~750ºC at ~30 kbar is obtained from a garnet core composition and a clinopyroxene core composition, whereas a consistent temperature-up estimate of ~850ºC at ~35 kbar is produced from a Grt (rim)–Cpx (rim) pair using the Grt-Cpx thermometers of Powell (1985), Krogh (1988), and Pattison and Newton (1989). The P-T estimates show that the peak UHP stage might comprise a near-peak UHP stage (IIa) and a real peak UHP stage (IIb). An obvious increase in both pressure and temperature is indicated from the near-peak to the peak UHP stage. This is compatible with prograde mineral zoning preserved in coarse garnet and clinopyroxene grains and in phengite flakes.

Post-peak retrograde stage (III-IV)

The retrograde stage is characterized by the development of symplectite assemblages such as amphibole-plagioclase on peak clinopyroxene, biotite-plagioclase, and K-feldspar-albite on phengite, and thin coronas of amphibole on garnet and ilmenite on rutile. Based on the Amp-Pl thermometer of Blundy and Holland (1990), we obtained a post-peak P-T condition at 7–9 kbar and 530–560ºC for an equilibrated symplectite assemblage of amphibole-plagioclase on peak clinopyroxene in the rutile eclogite sample B45-a (Table 2). A post-peak initial stage (III) is only inferred. In this case, a much lower P-T estimate of 530–560ºC at 7–9 kbar from symplectite assemblage of amphibole-plagioclase was obtained, which may reflect the conditions of a late retrograde metamorphic stage (IV).

The above P-T estimates agree with the results (700–890ºC and 28–40 kbar) obtained for the eclogites from other parts of the Sulu UHP terrane (R. Y. Zhang et al., 1995; Z. Zhang et al., 2000). Consequently, possible prograde and retrograde P-T paths for the UHP eclogite from the main hole of CCSD may be derived (Fig. 5). For instance, inasmuch as phengite eclogite (sample B854-a) was crustally derived, an initial prograde low P-T part (I) may be inferred, and thus rutile and phengite eclogites might have experienced distinct pre-peak initial prograde P-T stages (Fig. 5A). However, due to lack of constraints of assemblages and textures on the path between I and IIa for the rutile eclogite (sample B45-a), the initial prograde P-T stage of near isothermal increasing pressure or first temperature decrease, then pressure increase is uncertain (Fig. 5A). The P-T estimates from core and rim compositions of prograde mineral zonation indicate that both rutile and phengite eclogite underwent near-peak prograde heating accompanied by an increase in pressure, to attainment of the real peak UHP stage (IIb), but the rutile eclogite experienced a higher temperature and a slightly higher pressure with respect to phengite eclogite. Although post-peak P-T evolution is not well constrained, a post-peak decompression accompanied by cooling can be inferred for rutile and phengite eclogite, because they probably experienced similar post-peak retrograde processes during exhumation of the UHP terrane. The inferred post-peak P-T path is also compatible with other well-constrained post-peak evolution (e.g., Zhang et al., 1995).

Nevertheless, an alternative P-T path for the rutile and phengite eclogites could be constructed, if the euhedral amphibole inclusions in garnet grains formed as part of post-peak retrograde assemblages due to the development of fractures in the host garnets. If so, the P-T estimates of ~910ºC and ~13 kbar might reflect post-peak P-T conditions for a first retrograde stage (III) (Fig. 5B). In this case, rutile and phengite eclogites followed the same pre-peak prograde and retrograde P-T paths with nearly isothermal post-peak decompression followed by near isobaric cooling (Fig. 5B). Banno et al. (2000) suggested that eclogites from the northern Sulu belt experienced a post-peak retrograde P-T path of near isothermal decompression and passed through the granulite facies field. However, there is also

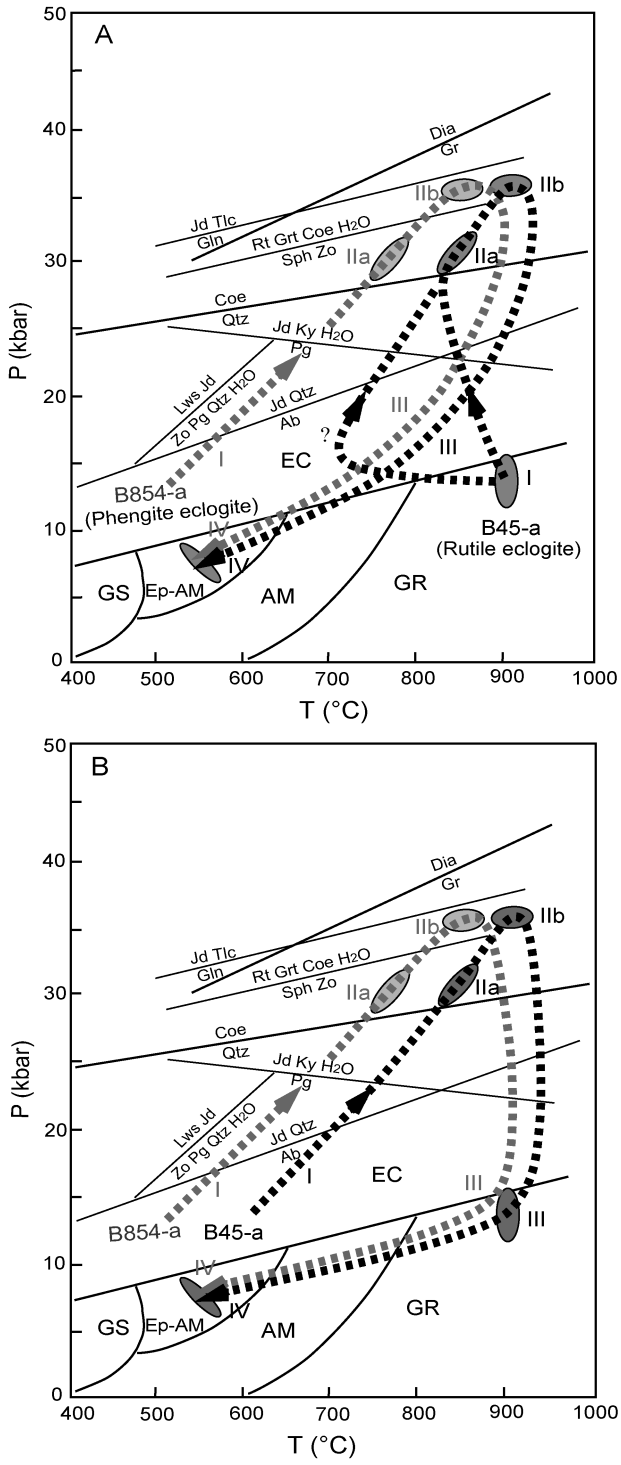


FIG. 5. *See following page for caption.*

FIG. 5. (*from preceeding page*) Possible P-T paths experienced by the rutile and phengite eclogites from the main CCSD borehole in Donghai (modified after R. Y. Zhang et al., 1995). A. P-T paths with different initial prograde stages for rutile and phengite eclogites. B. Similar P-T paths for rutile and phengite eclogites, assuming the amphibole inclusion as part of post-peak assemblages. Abbreviations: Ep-AM = epidote amphibolite; AM = amphibolite; EC = eclogite; GR = granulite. Reaction lines: Dia = Gr, after Bundy (1980); Rt + Grt + Coe + H2O = Sph + Zo, after Harley and Carswell (1995).

evidence for different thermal histories between the eclogites from the southern Sulu belt (CCSD locality) and the northern Sulu belt, and the southern Sulu belt did not experience a granulite-facies overprinting during the retrograde metamorphic stage (e.g., Yang, 2004). Therefore, we consider the first P-T path shown in Figure 5A more likely.

Furthermore, the following considerations support our preference above. (1) Small euhedral amphibole inclusion should be part of the pre-peak assemblages rather than the retrograde assemblages, because no retrograde symplectite assemblages occur along fractures. (2) Amphibole may be stable up to ~900 ºC at upper-mantle conditions (Ernst, 1999), and the amphibole inclusion in the garnet is similar in composition to the mantle-derived amphibole reported by R. Y. Zhang et al. (2005), and thus it may be mantle-derived. This is also compatible with the suggestion that rutile eclogite in the CCSD main hole is mantle-derived (You et al., 2004). (3) The high temperature of ~910ºC is also consistent with upper-mantle conditions. (4) The amphibole inclusion in garnet as part of pre-peak assemblages is compatible with the preservation of prograde growth zonation.

The rapid subduction and post-peak fast exhumation is likely responsible for the preservation of pre-peak inclusion assemblages and prograde mineral growth zonation, as a result of continental collision of the North China and Yangtze blocks during the Triassic (210–230 Ma). The presence of post-peak hydrous mineral assemblages may be attributed to metasomatism through fluid input during the retrograde metamorphic stage. In addition, rutile eclogite at upper structural levels shows higher temperature conditions than phengite eclogite at lower levels, suggesting that overthrusting may have occurred for different UHP eclogite slabs attending subduction.

Conclusions

The present study reveals that the eclogites from the CCSD main hole (100–2000 m) underwent three major metamorphic evolutionary stages: prograde, peak UHP, and retrograde stages.

1. The pre-peak stage is marked by small paragonite and euhedral amphibole inclusion assemblages in coarse-grained peak assemblages in rutile eclogite. P-T conditions of the pre-peak stage (I) are estimated as ~910ºC and ~13 kbar.

2. The peak UHP stage (II) is dominated by the development of the equilibrated assemblage of Grt + Cpx/Omp + Phn + Rt + Ap + Coe/Qtz pseudomorphs ± Ky. P-T conditions of the near-peak stage (IIa) are ~860ºC and ~30 kbar for rutile eclogite, and ~750ºC and ~28 kbar for phengite eclogite, respectively, whereas P-T conditions of the peak UHP stage (IIb) are ~910ºC and ~37 kbar for rutile eclogite, and ~850ºC and ~35 kbar for phengite eclogite.

3. The post-peak stage is related to the formation of decompression textures via back reactions, such as fine-grained symplectites of Amp-Pl on clinopyroxene/omphacite and Bt-Pl on phengite, and thin coronas of amphibole or zoisite on garnet and ilmenite on rutile. P-T conditions of the post-peak stage (IV) are 530–560ºC and 7–9 kbar.

4. The presence of K-feldspar–Ab symplectite on phengite, and minor interstitial K-feldspar implies that post-peak decompressional partial melting might have occurred locally during the rapid exhumation of subducted UHP slab.

5. Two types of P-T path have been derived for rutile and phengite eclogites. The first type shows distinct pre-peak evolutionary stages but compatible near-peak to post-peak decompression-cooling paths. The second type indicates that they might have had a shared P-T path from the pre-peak stage through the peak UHP stage to the post-peak stage of initial near-isothermal decompression, and subsequent near-isobaric cooling. The first set of P-T paths is preferred here, inasmuch as it is consistent with preservation of prograde mineral growth zoning, and an increase in pressure and temperature from near-peak to peak UHP stage.

Consequently, this research for the assemblages and textures of eclogites from the CCSD main hole suggests that subducting crustal slabs suffered *in situ* Triassic subduction-zone UHP metamorphism resulting from continental deep subduction and collision between the North China and Yangtze blocks.

Acknowledgments

We are grateful for the opportunity provided by Prof. W.G. Ernst to attend the Liou Symposium held at Stanford (9–10 December 2005). This paper is dedicated to Prof. J. G. Liou at his official retirement. Mr. Y.-C. Yang is thanked for his help with the laser Raman spectrometric analyses. A valuable discussion of inclusion assemblages and textures was undertaken with Dr. K. Okamoto during the initial preparation of the paper. Dr. R.Y. Zhang gave constructive comments on an early draft of this paper. We thank Dr. G. Zellmer for reading through the text carefully so that the exposition is much improved. This study is supported by NSC projects of Taiwan (NSC-93-2116-M-001-022, NSC-94-2116-M-001-088).

REFERENCES

Ames, L., Zhou, G., and Xiong, B., 1996, Geochronology and isotopic character of ultrahigh-pressure metamorphism with implications for collision on Sino-Korean and Yangtze cratons, central China: Tectonics, v. 15, p. 472–489.

Ayer, J. C., Dunkle, S., Gao, S., and Miller, C.F., 2002, Constraints on timing to peak and retrograde metamorphism in the Dabie Shan ultrahigh-pressure metamorphic belt, east-central China, using U-Th-Pb dating of zircon and monazite: Chemical Geology, v. 186, p. 315–331.

Banno, S., Enami, M., Hirajima, T., Ishiwatari, A., and Wang, Q. C., 2000, Decompression P-T path of coesite eclogite to granulite from Weihai, eastern China: Lithos, v. 52, p. 97–108.

Blundy, J. D., and Holland, T. J. B., 1990, Calcic amphibole equilibria and a new amphibole plagioclase thermometer: Contributions to Mineralogy and Petrology, v. 104, p. 208–224.

Bundy, F. R., 1980, The P, T phase and reaction diagram for elemental carbon: Journal of Geophysical Research, v. 31, p. 1353–1378.

Carswell, D. A., and Zhang, R. Y., 2000, Petrographic characteristics and metamorphic evolution of ultrahigh-pressure eclogites in plate-collision belts, *in* Ernst, W. G., and Liou, J. G., eds., Ultrahigh-pressure metamorphism and geodynamics in collision-type orogenic belts: Final report of the Task Group III-6 of the International Lithosphere Project, v. 4, p. 39–56.

Chavagnac, V., and Jahn, B. M., 1996, Coesite-bearing eclogites from the Bixiling Complex, Dabie Mountains, China: Sm-Nd ages, geochemical characteristics, and tectonic implications: Chemical Geology, v. 133, p. 29–51.

Coleman, R. G., and Wang, X., 1995, Overview of the geology and tectonics of UHPM, *in* Coleman, R. G., and Wang, X., eds., Ultrahigh-pressure metamorphism: Cambridge, UK: Cambridge University Press, p. 1–32.

Cong, B., Zhai, M., Carswell, D. A., Wilson, R. N., Wang, Q., Zhao, Z., and Windley, B. F., 1995, Petrogenesis of ultrahigh-pressure rocks and their country rocks at Shuanghe in Dabieshan, central China: European Journal of Mineralogy, v. 7, p. 119–138.

Cong, B., Zhang, R., Liou, J. G., Ye, K., and Wang, Q., 1996, Metamorphic evolution of UHPM rocks, *in* Cong, B., ed., Ultrahigh-pressure metamorphic rocks in the Dabieshan-Sulu Region of China: Beijing, China, Science Press, p. 128–160.

Enami, M., Zang, Q., and Yin, Y., 1993, High-pressure eclogites in northern Jiangsu–southern Shandong province, eastern China: Journal of Metamorphic Geology, v. 11, p. 589–603.

Ernst, W. G., 1999, H_2O and ultrahigh-pressure subsolidus phase relations for mafic and ultramafic systems: International Geology Review, v. 41, p. 886–894.

Ernst, W. G., and Liou, J. G., 1995, Contrasting plate-tectonic styles of the Qingling-Dabie-Sulu (Alpine-type) and Franciscan (Pacific-type) metamorphic belts: Geology, v. 23, p. 353–356.

Ernst, W. G., and Liou, J. G., 2000, Overview of UHP metamorphism and tectonics in well-studied collisional orogens, *in* Ernst, W. G., and Liou, J. G., eds., Ultrahigh-pressure metamorphism and geodynamics in collision-type orogenic belts: Final report of the Task Group III-6 of the International Lithosphere Project, v. 4, p. 3–19.

Faure, M., Lin, W., and Breton, N. L., 2001, Where is the North China–South China block boundary in eastern China?: Geology, v. 29, p. 119–122.

Graham, C. M., and Powell, R., 1984, A garnet-hornblende geothermometer: Calibration, testing and application to the Pelona Schist, Southern California: Journal of Metamorphic Geology, v. 2, p. 13–31.

Hacker, B. R., Ratschbacher, L., Webb, L., and Dong, S., 1995, What brought them up? Exhumation of the Dabieshan ultrahigh-pressure rocks: Geology, v. 23, p. 743–746.

Hacker, B. R., Ratschbacher, L., Webb, L., Ireland, T., Walker, D., and Dong, S., 1998, U/Pb zircon ages constrain the architecture of the ultrahigh-pressure Qinling-Dabie Orogen, China: Earth and Planetary Science Letters, v. 161, p. 215–230.

Hacker, B. R., Ratschbacher, L., Webb, L., McWilliams, M. O., Ireland, T., Calvert, A., Dong, S., Wenk, H.-R., and Chateigner, D. Q., 2000, Exhumation of ultrahigh-pressure continental crust in east-central China: Late Triassic–Early Jurassic tectonic unroofing: Journal of Geophysical Research, v. 105, p. 13,339–13,364.

Hammarstrom, J. M., and Zen, E. A., 1986, Aluminium in hornblende: An empirical igneous geobarometer: American Mineralogist, v. 71, p. 1297–1313.

Harley, S. L., and Carswell, D. A., 1995, Ultradeep crustal metamorphism: A prospective view: Journal of Geophysical Research, v. 100, p. 8367–8380.

Hirajima, T., Ishiwatari, A., Cong, B., Zhang, R., Banno, S., and Nozaka, T., 1990, Coesite from Mengzhong eclogite at Donghai county, northeastern Jiangsu Province, China: Mineralogical Magazine, v. 54, p. 579–583.

Hollister, L. S., Grison, G. C., Peters, E. K., Stowell, H. H., and Sisson, V. B., 1987, Confirmation of the empirical correlation of Al in hornblende with pressure of solification of calc-alkaline plutons: American Mineralogist, v. 72, p. 231–239.

Jahn, B. M., Fan, Q., Yang, J. J., and Henin, O., 2003a, Petrogenesis of the Maowu pyroxenite-eclogite body from the UHP metamorphic terrane of Dabieshan: Chemical and isotopic constraints: Lithos, v. 70, p. 243–267.

Jahn, B. M., Rumble, D., and Liou, J. G., 2003b, Geochemistry and isotope tracer study of UHP metamorphic rocks, *in* Carswell, D. A., and Compagnoni, R., eds., Ultrahigh pressure metamorphism: EMU Notes in Mineralogy, v. 5, p. 365–414.

Johnson, M. C., and Rutherford, M. J., 1989, Experimental calibration of the aluminium-in-hornblende geobarometer with application to Long Valley (California) volcanic rocks: Geology, v. 17, p. 837–841.

Kretz, R., 1983, Symbols for rock-forming minerals: American Mineralogist, v. 68, p. 277–279.

Krogh, E. G., 1988, The garnet-clinopyroxene Fe-Mg geothermometer—a reinterpretation of existing experimental data: Contributions to Mineralogy and Petrology, v. 99, p. 44–48.

Leake, B. E., Wolley, A. R., Arps, C. E. S. et al., 1997, Nomenclature of Amphiboles: Report of the Subcommittee on Amphiboles of the International Mineralogical Association Commission on New Minerals and Mineral Names: Mineralogical Magazine, v. 61, p. 295–321.

Li, S., Chen, Y., Cong, B., Zhang, Z., Zhang, R. Y., Liu, D., Hart, S. R., and Ge, N., 1993, Collision of the North China and Yangtze blocks and formation of coesite-bearing eclogites: Timing and processes: Chemical Geology, v. 109, p. 70–89.

Li, S., Jagoutz, E., Xiao, Y. L., Ge, N. J., and Chen, Y. Z., 1996, Ultrahigh-pressure metamorphic chronology of the Sulu-Dabieshan terrane: Sm-Nd isotope system: Science in China (series D), v. 26, p. 249–257.

Liou, J. G., Banno, S., and Ernst, W. G., 1995, Ultrahigh-pressure metamorphism and tectonics: The Island Arc, v. 4, p. 233–239.

Liou, J. G., Tsujimori, T., Zhang, R. Y., Katayama, I., and Maruyama, S., 2004, Global UHP metamorphism and continental subduction/collision: The Himalayan model: International Geology Review, v. 46, p. 1–27.

Liou, J. G., Zhang, R. Y., and Ernst, R. G., 1994, Introduction to ultrahigh-pressure metamorphism: The Island Arc, v. 3, p. 1–24.

Liou, J. G., Zhang, R. Y., Ernst, W. G., Rumble, D., and Maruyama, S., 1998, High- pressure minerals from deeply subducted metamorphic rocks, *in* Hemley, R. J., ed., Ultrahigh-pressure mineralogy: Physics and chemistry of the Earth's deep interior: Reviews in Mineralogy, v. 37, p. 33–96.

Liou, J. G., Zhang, R. Y., and Jahn, B. M., 1997, Petrology, geochemistry and isotope data on a ultrahigh-pressure jadeite quartzite from Shuanghe, Dabie Mountains, East-central China: Lithos, v. 41, p. 59–78.

Liu, F., Liou, J. G., and Xu, Z., 2005, U-Pb SHRIMP ages recorded in the coesite-bearing zircon domains of paragneisses in the southwestern Sulu terrane, eastern China: New interpretation: American Mineralogist, v. 90, p. 790–800.

Liu, F., Xu., Z., Liou, J. G., Katayama, I., Masago, H., Maruyama, H., and Yang, J. S., 2002, Ultrahigh-pressure mineral inclusions in zircons from gneissic core samples of the Chinese Continental Scientific Drilling Site in eastern China: European Journal of Mineralogy, v. 14, p. 499–512.

Liu, F., Xu., Z., Liou, J. G., and Song, B., 2004a, SHRIMP U-Pb ages of ultrahigh- pressure and retrograde metamorphism of gneisses, south-western Sulu terrane, eastern China: Journal of Metamorphic Geology, v. 22, p. 315–326.

Liu, F. L., Xu., Z. Q., Yang, J. S., Zhang, Z. M., Xue, H. M., and Li, T. F., 2004b, Geochemical characteristics and UHP metamorphism of granitic gneisses in the main drilling hole of Chinese Continental Scientific Drilling Project and its adjacent area: Acta Petrologica Sinica, v. 20, p. 9–26 (in Chinese).

Liu, J., Ye, K., Maruyama, S., Cong, B., and Fan, H., 2001, Mineral inclusions in zircon from gneisses in the ultrahigh-pressure zone of the Dabie mountains, China: Journal of Geology, v. 109, p. 523–535.

Massone, H. J., and Schreyer, W., 1989, Stability field of the high-pressure assemblage talc + phengite and two new phengite barometers: European Journal of Mineralogy, v. 1, p. 391–410.

Okay, A. I., 1993, Petrology of a diamond and coesite-bearing metamorphic terrane: Dabie Shan, China: European Journal of Mineralogy, v. 5, p. 659–673.

Okay, A. I., Xu, S., and Sengor, A. M. C., 1989, Coesite from the Dabie Shan eclogites, central China: European Journal of Mineralogy, v. 1, p. 595–598.

Pattison, D. R. M., and Newton, R. C., 1989, Reversed experimental calibration of the garnet-clinopyroxene thermometer: Contributions to Mineralogy and Petrology, v. 101, p. 87–103.

Perchuk, L. L., Aranovich, L. Y., and Kitsul, V. I., 1985, Precambrian granulites of the Aldan shields, eastern

Siberia, USSR: Journal of Metamorphic Geology, v. 3, p. 265–310.

Powell, R., 1985, Regression diagnostic and robust regression in geothermometer/geobarometer calibration: The garnet-clinopyroxene geothermometer revisited: Journal of Metamorphic Geology, v. 3, p. 231–243.

Rumble, D., and Yui, T. F., 1998, The Qinglongshan oxygen and hydrogen isotope anomaly near Donghai in Jiangsu province, China: Geochimica et Cosmochimica Acta, v. 62, p. 3307–3321.

Schertl, H., and Okay, A. I., 1994, Coesite inclusion in dolomite of Dabie Shan, China: Petrological and geological significance: European Journal of Mineralogy, v. 6, p. 995–1000.

Wallis, S., Enami, M., and Banno, S., 1999, The Sulu UHP terrane—a review of the petrology and structural geology: International Geology Review, v. 41, p. 906–920.

Wang, Q., Ishiwatari, A., Zhao, Z., Hirajima, T., Hiramatsu, N., Enami, M., Zhai, M., Li, J., and Cong, B., 1993, Coesite-bearing granulite retrograded from eclogite in Weihai, eastern China: European Journal of Mineralogy, v. 5, p. 141–152.

Wang, X., and Liou, J., 1991, Regional ultrahigh-pressure coesite-bearing eclogitic terrane in central China: Evidence from country rocks, gneiss, marble, and metapelite: Geology, v. 19, p. 933–936.

Wang, X., Liou, J., and Mao, H. K., 1989, Coesite-bearing eclogite from the Dabie Mountains in central China: Geology, v. 17, p. 1085–1088.

Wang, X., Liou, J., and Maruyama, S. 1992, Coesite-bearing eclogites from the Dabie Mountains, central China: Petrogenesis, P-T paths, and implications for regional tectonics: Journal of Geology, v. 100, p. 231–250.

Xu, S., Liu, Y., Chen, G., Ji, S., Ni, P., and Xiao, W., 2005, Microdiamonds, their classification and tectonic implications for the host eclogites from the Dabie and Su-Lu regions in central eastern China: Mineralogical Magazine, v. 69, p. 509–520.

Xu, S., Okay, A.I., Ji, S., Sengor, A. M. C., Su, W., Liu, Y., and Jiang, L., 1992, Diamond from the Dabie Shan metamorphic rocks and its implication for tectonic setting: Science, v. 256, p. 80–82.

Xu, Z. Q., Zhang, Z. M., Liu, F. L., Yang, J. S., Tang, Z. M., Chen, S. Z., Cai, Y. C., Li, T. F., and Cheng, F. Y., 2004, The structural profile of 0–2000 m in the main hole, Chinese Continental Scientific Drilling and its preliminary deformation analysis: Acta Petrologica Sinica, v. 20, p. 53–72 (in Chinese).

Xue, F., Rowley, D. B., and Baker, J., 1996, Refolded syn-ultrahigh-pressure thrust sheets in the southern Dabie complex, China: Field evidence and tectonic implications: Geology, v. 24, p. 455–458.

Yang., J. J., Godard, G., Kienast, J.-R., Lu, Y., and Sun, J., 1993, Ultrahigh-pressure (60 kbar) magnesite-bearing garnet peridotites from northeastern Jiangsu, China: Journal of Geology, v. 101, p. 541–554.

Yang., J. J., and Jahn, B. M., 2000, Deep subduction of mantle-derived garnet peridotites from the Su-Lu UHP metamorphic terrane in China: Journal of Metamorphic Geology, v. 18, p. 167–180.

Yang, T. N., 2004, Retrograde textures and associated mass transfer: Evidence for aqueous fluid action during exhumation of the Qinglongshan eclogite, Southern Sulu ultrahigh pressure metamorphic terrane, eastern China: Journal of Metamorphic Geology, v. 22, p. 653–669.

Yao, Y., Ye, K., Liu, J., Cong, B., and Wang, Q., 2000, A transitional eclogite- to high pressure granulite–facies overprint on coesite-eclogite at Taohang in the Sulu ultrahigh-pressure terrane, Eastern China: Lithos, v. 52, p. 109–120.

Ye, K., Cong, B., and Ye, D., 2000a, The possible subduction of continental materials to depths greater than 200 km: Nature, v. 407, p. 734–736.

Ye, K., Yao, Y., Katayama, I., Cong, B., Wang, Q., and Maruyama, S., 2000b, Large areal extent of ultrahigh pressure metamorphism in the Sulu UHP terrain of eastern China: New implications from coesite and omphacite inclusions in zircon of granitic gneiss: Lithos, v. 52, p. 157–164.

Ye, K., Liou, J., Yao, Y., Cong, B., and Wang, Q., 2001, Dehydration melting of phengite during early stage exhumation of coesite eclogites from the Sulu ultrahigh-pressure terrane, eastern China [abs.], *in* 6th International Eclogite Conference, Volume Conference Abstracts: Niihama, Japan, p. 179.

You, Z. D., Su, S. G., Liang, F. H., and Zhang, Z. M., 2004, Petrography and metamorphic deformational history of the ultrahigh-pressure metamorphic rocks from the 100–2000 m core of Chinese Continental Scientific Drilling, China: Acta Petrologica Sinica, v. 20, p. 43–52 (in Chinese).

Yui, T. F., Rumble, D., and Lo, C. H., 1995, Unusually low $\delta^{18}O$ ultrahigh-pressure metamorphic rocks from the Sulu terrain, eastern China: Geochimica et Cosmochimica Acta, v. 59, p. 2859–2864.

Zhang, R. Y., Hirajima, T., Banno, S., Cong, B., and Liou, J. G., 1995, Petrology of ultrahigh-pressure rocks from the southern Su-Lu region, eastern China: Journal of Metamorphic Geology, v. 13, p. 659–675.

Zhang, R. Y., and Liou, J. G., 1999, Exsolution lamellae in minerals from ultrahigh-pressure rocks: International Geology Review, v. 41, p. 981–993.

Zhang, R. Y., Liou, J. G., and Cong, B., 1994, Petrogenesis of garnet-bearing ultramafic rocks and associated eclogites in the Su-Lu UHP terrane, eastern China: Journal of Metamorphic Geology, v. 12, p. 169–186.

Zhang, R. Y., Liou, J. G., Yang, J. S., and Yui, T. F., 2000, Petrochemical constraints for dual origin of garnet peridotites from the Dabie-Sulu UHP terrane, eastern-

central China: Journal of Metamorphic Geology, v. 18, p. 149–166.

Zhang, R. Y., Liou, J. G., Zheng, Y. F., and Fu, B., 2003, Transition of UHP eclogites to gneissic rocks of low-amphibolite facies during exhumation: evidence from the Dabie terrane, central China: Lithos, v. 70, p. 269–291.

Zhang, R.Y., Liou, J.G., Zheng, J.P., Griffin, W.L., Yui, T. F., and O'Reilly, S.Y., 2005, Petrogenesis of the Yangkou layered garnet-peridotite complex, Sulu UHP terrane, China: American Mineralogist, v. 90, p. 801–813.

Zhang, Z., Xiao, Y., Liu, F., Liou, J. G., and Hoefs, J., 2005, Petrogenesis of UHP metamorphic rocks from Qinglongshan, southern Sulu, east-central China: Lithos, v. 81, p. 189–207.

Zhang, Z., Xu, Z., and Xu, H., 2000, Petrology of ultra-high-pressure eclogites from the ZK703 drillhole in the Donghai, eastern China: Lithos, v. 52, p. 35–50.

Zhang, Z. M., Xu, Z. Q., Liu, F. L., You, Z. D., Shen, K., Yang, J. S., Li, T. F., and Chen, S. Z., 2004, Geoochemistry of eclogites from the main hole (100–2050 m) of the Chinese Continental Scientific Drilling Project: Acta Petrologica Sinica, v. 20, p. 27–42 (in Chinese).

Zhao, Z. Y., Fang, A. M., and Yu., L. J., 2003, High- to ultrahigh-pressure (UHP) ductile shear zones in the Sulu UHP metamorphic belt, China: Implications for continental subduction and exhumation: Terra Nova, v. 15, p. 322–329.

Zheng, Y. F., Fu, B., Cong, B., and Li, S., 1996, Extreme $\delta^{18}O$ depletion in eclogite from the Su-Lu terrane in east China: European Journal of Mineralogy, v. 8, p. 317–323.